Modifications of local structures of Gd_2O_3 on incorporation of SiO_2

N. C. Das,[1] N. K. Sahoo,[1] D. Bhattacharyya,[1,a)] S. Thakur,[1] D. Nanda,[2] S. Hazra,[3] J. K. Bal,[3] J. F. Lee,[4] Y. L. Tai,[4] and C. A. Hsieh[4]

[1]*Applied Spectroscopy Division, Bhabha Atomic Research Centre, Trombay, Mumbai 400085, India*
[2]*Coolant Systems Laboratory, Raja Ramanna Centre for Advanced Technology, Indore 452013, India*
[3]*Surface Physics Division, Saha Institute of Nuclear Physics, 1/AF Bidhannagar, Kolkata 700064, India*
[4]*National Synchrotron Radiation Research Center, 101 Hsin-Ann Road, Hsinchu Science Park, Hsinchu 30076, Taiwan*

(Received 14 March 2011; accepted 18 August 2011; published online 27 September 2011)

In the present work we have reported the results of investigations on local structures of e-beam evaporated (Gd_2O_3-SiO_2) composite thin films by synchrotron based EXAFS measurements. The evolution of local structure in the case of the Gd_2O_3-SiO_2 system is found to be different from the HfO_2-SiO_2 system reported by us earlier. The EXAFS analysis has shown that the Gd-O bond length decreases monotonically as SiO_2 content in the films increases. Also the amplitudes of the peaks in the FT-EXAFS spectra of the samples, which depend jointly on the coordination numbers as well as the Debye-Waller factors (measure of disorder) are found to decrease monotonically with increase in SiO_2 contents in the Gd_2O_3 matrix. Atomic force microscopy (AFM) measurements of the samples also show continuous evolution of amorphous-like denser microstructure with increase in SiO_2 content in the films. Hence incorporation of SiO_2 in the Gd_2O_3 matrix, results in a continuous change in oxygen coordination yielding a change in the Gd-O bond length and also results in a continuous increase in amorphousness and a smoother morphology of the samples and, unlike the HfO_2-SiO_2 system, does not show any maximum for a particular SiO_2 concentration. © *2011 American Institute of Physics*. [doi:10.1063/1.3642083]

I. INTRODUCTION

Gadolinium oxide (Gd_2O_3) has been identified as a very useful material for the semiconductor industry and optical coating technology.[1] High-k dielectric Gd_2O_3 has been extensively used as low leakage current gate dielectric in the development of GaAs based metal oxide semiconductor (MOS) diodes[2,3] and GaAs and GaN based metal-oxide-semiconductor field-effect transistors (MOSFETs).[4–7] It has also been demonstrated that epitaxial Gd_2O_3 films developed as the gate dielectrics for Si are comparable to the state-of-the-art SiO_2 gate oxide due to very low leakage current.[8]

Because of its high refractive index and extended transparency from the ultraviolet to infrared region of the spectrum,[9] Gd_2O_3 has also proven its importance as a high refractive index coating material in optical thin film technology. In a series of publications,[10–14] we have reported the dependence of various structural and optical properties, viz., surface topographies, microstuctures, viscoelasticity, bandgap, refractive index etc., of reactive electron beam deposited thin film optical coatings of Gd_2O_3 on different process parameters, namely, reactive oxygen pressure, deposition rate, substrate temperature etc. Using the optimized process parameters for thin films of Gd_2O_3 and SiO_2, several types of multilayer high reflection filters have been developed[11] for ultraviolet and deep ultraviolet laser wavelengths.

Composite thin films consisting of high-index and low-index materials deposited through a co-deposition technique have gained significant importance in the optical coating technology because of their refractive index tunability property. This has enabled one to design thin film devices with minimum number of layers in the stack. In our earlier communication,[15,16] we have reported the refractive index and bandgap tunability in e-beam deposited composite (Gd_2O_3-SiO_2) thin films. Composite films of Gd_2O_3-SiO_2[15,16] have shown superior micro-structural and morphological properties as compared to those of pure Gd_2O_3 thin film and have shown better potential as high-k dielectric material and high refractive index material for fabrication of multilayer dielectric coatings.

Retention of the amorphousness of the composite films is an important criterion for its application in both as high-k dielectric and optical multiulayers, since amorphous structure with small grain size leads to high density and high refractive index in thin films, which also helps in preventing the leakage current, and incorporation of SiO_2 has been found to help in retaining the amorphous phase in high-k dielectrics up to a relatively higher temperature.[17–20] We have in an earlier communication[21] investigated the microscopic reason for enhanced amorphousness and superior optical properties of the HfO_2-SiO_2 composite films by carrying out synchrotron-based extended x-ray absorption fine structure (EXAFS) measurements on these films. In the present communication, we have carried out EXAFS measurements on pure Gd_2O_3 and composite (Gd_2O_3-SiO_2) thin films and compared them with the previously reported results on HfO_2-SiO_2 composite films.

[a)]Author to whom correspondence should be addressed. Electronic mail: dibyendu@barc.gov.in.

 © 2011 American Institute of Physics

II. EXPERIMENTAL SECTION

The present set of Gd_2O_3-SiO_2 composite films with different Gd_2O_3 to SiO_2 ratios have been prepared by a reactive co-evaporation technique where 99.9% pure Gd_2O_3 and SiO_2 powders were evaporated simultaneously using two 8 kW electron beam guns on quartz substrates maintained at 350 °C.[11] The rates and thickness of the coatings were monitored *in situ* using Inficon's XTC/2 quartz crystal monitors and Leybold's OMS-2000 optical thickness monitors. High purity O_2 is bled into the system in a controlled fashion through a MKS mass flow controller to compensate for the dissociation of the oxide evaporants. The O_2 flow is controlled so that pressure inside the chamber remains constant at $\sim 1 \times 10^{-4}$ mbar during deposition.

EXAFS experiments on the above mentioned thin film samples were carried out at the BL17C1 beamline on the Taiwan Light Source (1.5 Gev, 300 mA) at the National Synchrotron Radiation Research Center, Hsinchu, Taiwan.[22] The beamline uses a Si(111) double crystal monochromator (DCM) and the measurements have been carried out in the fluorescence mode at the L_3 absorption-edge of gadolinium at 7.2 keV.

Grazing incidence x-ray diffraction (GIXRD) measurements on these films have been carried out using Cu K_α radiation in a versatile diffractometer (model D8, Discover, Bruker AXS). Because the measurements have been carried out on thin film samples the data were recorded by keeping the incident angle fixed at a grazing angle in order to keep the probing area of the sample near its surface.

III. RESULTS AND DISCUSSION

Figure 1 shows the absorption spectra ($\mu(E)$ versus E) of composite (Gd_2O_3-SiO_2) thin films with composition ratios of (100-0), (90-10), and (70-30), respectively. In order to take care of the oscillations in the absorption spectra, the energy dependent absorption coefficient $\mu(E)$ has been converted to the absorption function $\chi(E)$, defined as follows:[23]

$$\chi(E) = \frac{\mu(E) - \mu_0(E)}{\Delta\mu_0(E_0)} \tag{1}$$

where E_0 is absorption edge energy, $\mu_0(E)$ is the bare atom background, and $\Delta\mu_0(E_0)$ is the step in the $\mu(E)$ value at the absorption edge. After converting the energy scale to the photoelectron wave number scale (k), as defined by

$$k = \sqrt{\frac{2m(E - E_0)}{\hbar^2}} \tag{2}$$

the energy dependent absorption coefficient $\chi(E)$ has been converted to the wave number-dependent absorption coefficient $\chi(k)$, where m is the electron mass. Finally, $\chi(k)$ is weighted by k^2 to amplify the oscillation at high k and the $\chi(k)\,k^2$ functions are Fourier transformed in R space to generate the $\chi(R)$ versus R (or FT-EXAFS) spectra in terms of the real distances from the center of the absorbing atom.

Figures 2(a), 2(b), and 2(c) show the experimental $\chi(R)$ versus R spectra of composite (Gd_2O_3-SiO_2) thin films with composition ratios of (100-0), (90-10), and (70-30) respectively. It may be seen from Fig. 2 that the first shell peak intensity gradually decreases with the increase of SiO_2 percentage, and that there is a shifting of the second shell maxima. A similar type of local structure evolution with the grain size variation in (Gd_2O_3-HfO_2) and (Gd_2O_3-ZrO_2) nanocrystalline powders as marked by the first shell peak intensity variation as well as shifting of the second shell maxima in the $\chi(R)$ versus R spectra has been reported by Menushenkov *et al.*[24]

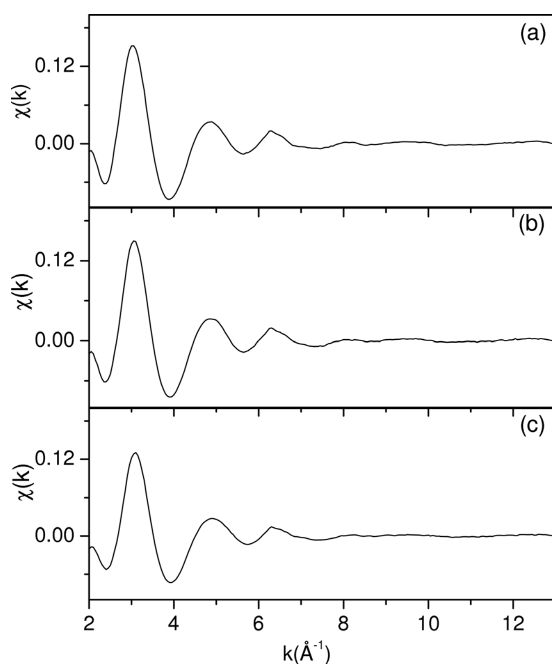

FIG. 1. μ vs E spectra of (Gd_2O_3-SiO_2) composite thin films with composition ratios of (a) (100-0), (b) (90-10), and (c) (70-30).

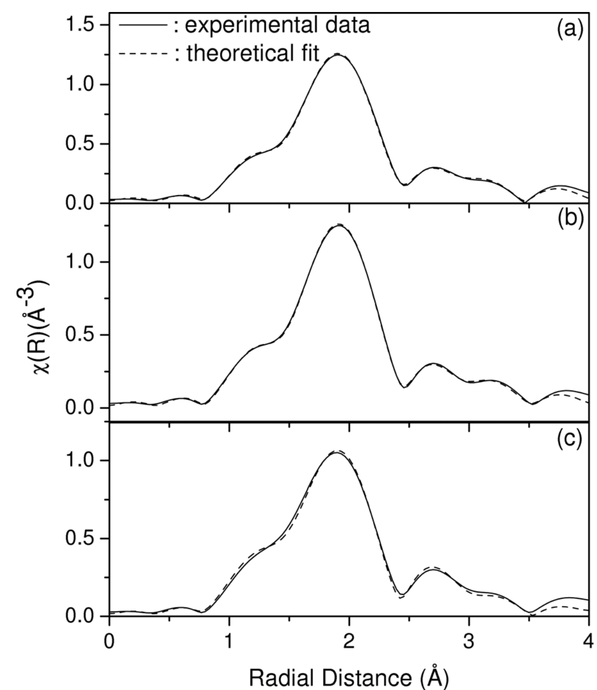

FIG. 2. Experimental $\chi(R)$ vs R spectra along with best-fit theoretical plots for (Gd_2O_3-SiO_2) composite thin films with composition ratios of (a) (100-0), (b) (90-10), and (c) (70-30).

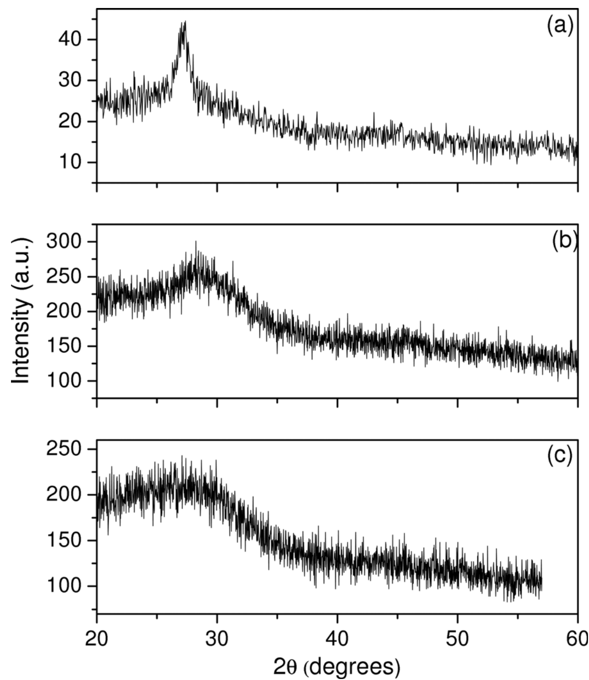

FIG. 3. GIXRD spectra of (a) pure Gd_2O_3 and (Gd_2O_3-SiO_2) composite thin films with composition ratios of (b) (90-10), and (c) (70-30).

As discussed in the previous section, the crystallinity of the samples has been investigated by grazing incidence x-ray diffraction (GIXRD) measurements on pure Gd_2O_3 and composite (Gd_2O_3-SiO_2) thin films. Figures 3(a), 3(b), and 3(c) show the GIXRD (θ-2θ scan) patterns of pure Gd_2O_3 and composite (Gd_2O_3-SiO_2) thin films having 10% and 30% silica contents respectively. It may be seen from Fig. 3(a) that the GIXRD pattern of pure Gd_2O_3 thin film consists of an amorphous-like broad peak indicating the absence of any crystalline structure in the film.[25] The addition of 10% silica has significantly broadened this peak (Fig. 3(b)), which confirms the increase of amorphousness in the composite thin film and the peak broadens further as SiO_2 content is increased to 30% (Fig. 3(c)).

It should be noted that the R axes in the above figures (Fig. 2) do not represent the actual distances from the absorbing atom; rather, they represent the distances without phase shift corrections and hence the peak positions do not exactly correspond to the bond distances. In order to obtain the actual quantitative information on the local structure variation of the composite (Gd_2O_3-SiO_2) thin film, the bond distance and coordination number of the neighboring atoms (N) around the Gd atom have been evaluated by fitting the experimental $\chi(R)$ versus R spectra with the theoretical spectra. It should be mentioned here that a set of EXAFS data analysis programs available within the IFEFFIT package was used for the above analysis.[26] This includes data reduction and Fourier transform to derive the $\chi(R)$ versus R spectra from the absorption spectra, generation of the theoretical EXAFS spectra starting from an assumed crystallographic structure, and, finally, fitting of the experimental data with the theoretical spectra using the FEFF 6.0 code. It may be mentioned that powder Gd_2O_3 mostly exists in monoclinic and cubic types of crystallographic phases.[27–29] Referring to Fig. 3(a), since the GIXRD spectrum of pure Gd_2O_3 thin film shows an amorphous-like broad feature, which broadens further as SiO_2 incorporation in Gd_2O_3 matrix is increased; the theoretical EXAFS spectra of pure Gd_2O_3 and composite (Gd_2O_3-SiO_2) thin films have been simulated assuming an amorphous nature of the samples. The bond distances, coordination numbers (including scattering amplitudes), and Debye-Waller factors (σ^2) specifying the mean-square fluctuations in the bond distances, have been used as the fitting parameters.

The best fitted $\chi(R)$ versus R spectra for the (Gd_2O_3-SiO_2) samples with composition ratios of (100-0), (90-10), and (70-30) respectively have also been shown in Figs. 2(a), 2(b), and 2(c) along with the experimentally derived spectra. As extracted from the fitting results, the peak with highest intensity corresponds to the (Gd-O) bond and the remaining two peaks correspond to two separate (Gd-Gd) bonds. The local structural parameters of the first two coordination shells around a Gd atom as extracted from the fitting have been summarized in Table I for various samples. It may be seen that (Gd-O) and (Gd-Gd) bond lengths (R), coordination number (N), and mean-square fluctuation (σ^2) in the bond distance change with the variation of SiO_2 composition in the thin film samples. It may be mentioned that the (Gd-O) bond length of pure Gd_2O_3 thin film is more or less similar to that of epitaxially grown Gd_2O_3 thin film as reported by Nelson and Woici.[30] It also may be seen that as the SiO_2 content increases from the zero value in the composite (Gd_2O_3-SiO_2) thin films, the Gd-O bond lengths decrease monotonically. The variation of (Gd-O) bond length with compositional change has also been reported by Nakagawa *et al.*[31] for the (Gd_2O_3-CeO_2) binary system. Figures 4(a) and 4(b) show the bond length variation with SiO_2 content in the composite (Gd_2O_3-SiO_2) thin film as obtained from EXAFS experiment. It can also be seen from Fig. 2 that the

TABLE I. Structural parameters bond length (R) and coordination number (N) corresponding to the first (Gd-O) and the second (Gd-Gd) coordination shells around a atom as obtained from EXAFS data analysis of pure Gd_2O_3 and (Gd_2O_3-SiO_2) composite.

Sample	Parameter	Gd_2O_3 (100%)	(Gd_2O_3-SiO_2) (90%-10%)	(Gd_2O_3-SiO_2) (80%-20%)	(Gd_2O_3-SiO_2) (70%-30%)
First coordination shell (Gd-O)	N (atoms)	8.71 ± 0.13	8.37 ± 0.11	8.04 ± 0.10	7.52 ± 0.11
	R(Å)	2.413 ± 0.007	2.409 ± 0.011	2.404 ± 0.006	2.389 ± 0.008
	σ^2(Å^2)	0.0128 ± 0.0015	0.0132 ± 0.0082	0.0120 ± 0.0012	0.0132 ± 0.0015
Second coordination shell (Gd-Gd)	N (atoms)	9.50 ± 0.18	9.31 ± 0.27	9.13 ± 0.35	7.56 ± 0.25
	R(Å)	3.244 ± 0.039	3.242 ± 0.058	3.245 ± 0.035	3.232 ± 0.036
	σ^2(Å^2)	0.0181 ± 0.0062	0.0697 ± 0.0104	0.0371 ± 0.0057	0.0317 ± 0.0055

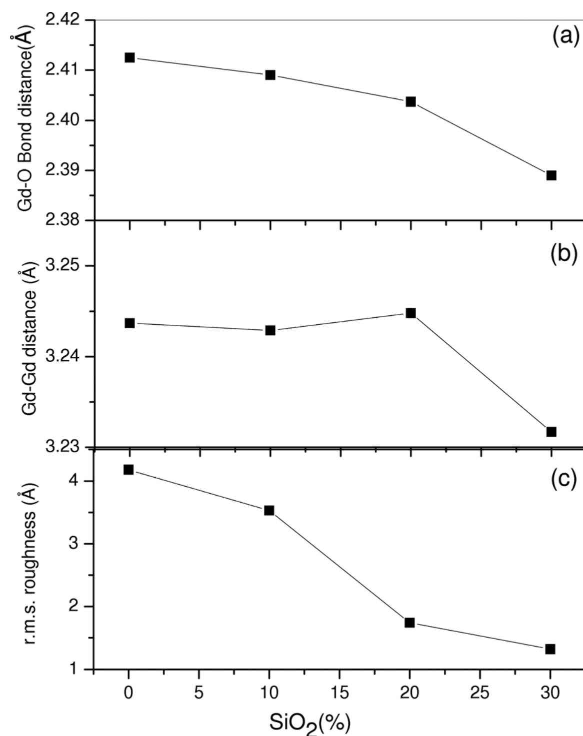

FIG. 4. (a) Variation of Gd-O bond length with the SiO_2 percentage in the (Gd_2O_3-SiO_2) composite thin films. (b) Variation of Gd-Gd bond length with the SiO_2 percentage in the (Gd_2O_3-SiO_2) composite thin films. (c) Variation of rms surface roughness with the SiO_2 percentage in the (Gd_2O_3-SiO_2) composite thin films.

decrease in bond length also accompanies a monotonic decrease in the amplitudes of the first and second peaks in the $\chi(R)$ versus R (FT-EXAFS) spectra of the samples.

The above trend of variation of Gd-O and Gd-Gd bond lengths for the Gd_2O_3-SiO_2 composite films are similar to the HfO_2-SiO_2 composite films reported earlier by us,[21] where also it had been observed that the amplitude of the first and second peaks in the $\chi(R)$ versus R (FT-EXAFS) spectra of the samples follow the same trend as the Hf-O and Hf-Hf bond lengths with the height of the peaks being minimum for the sample with 10% SiO_2, for which the bond lengths are also found to be minimum and the amplitudes of the peaks increase further along with the bond lengths with an increase in SiO_2 content in the films. Several other authors[32–35] have also reported the change in oxygen coordination surrounding Hf atoms due to incorporation of more covalent SiO_2 in ionic HfO_2 lattice, while Cho *et al.*[36] have indicated that creation of oxygen vacancies surrounding Hf atoms change the Hf-O bond lengths along with the O-coordination due to rearrangement of Coulombic interactions. In other words, for HfO_2-SiO_2 and Gd_2O_3-SiO_2 composite thin film system, the change in bond lengths is associated with the change in oxygen coordination of Hf and Gd atoms.

However, apart from the coordination number, amplitudes of the peaks in FT-EXAFS spectra also include the effect of disorder through the Debye-Waller factor term (σ^2) and, from the GIXRD measurements on the samples, as discussed above, we have observed an increase in amorphousness in the samples with an increase in SiO_2 content. It should also be mentioned here that for Gd_2O_3-SiO_2 composite films, rms roughness obtained from atomic force microscopy (AFM) measurements decreases monotonically (implying evolution of more amorphous-like denser morphology) with an increase in silica content, as shown in Fig. 4(c). Although AFM measurement does not directly yield information regarding crystallinity of samples, it is well established in the literature that surface roughness of polycrystalline films, irrespective of the preparation methods, increases as crystallinity of the samples improves because of the evolution of grain structures. For example, Tang *et al.*[37] have observed for their sol-gel deposited $PbZrO_3$ films, that the rms roughness increases from 0.4 nm for an amorphous film to 1.2 nm for a well-crystallized film. Park *et al.*[38] have observed a sharp increase in rms roughness as the AFM tip enters from the amorphous region to the crystalline region for their organic rubrene thin films. Similar results of an increase in surface roughness with improvement in crystallinity were observed for rf magnetron sputter deposited Ta_2O_5 films by Lee *et al.*[39] and Huang *et al.*[40] Surface roughness of crystalline $Ba_{0.5}Sr_{0.5}TiO_3$ films deposited by laser ablation[41] and of thermal plasma deposited ZnO films[42] was observed to be significantly higher than their amorphous counterparts. Hence the EXAFS measurement results on our Gd_2O_3-SiO_2 composite films show that with an increase in SiO_2 content in the films, along with the change in oxygen coordination, which results in a decrease in bond lengths and height in the Gd-O peaks in the $\chi(R)$ versus R spectra of the samples, the morphology of the samples also becomes more and more smooth because of a gradual increase in amorphousness in the composite films.

The above results agree with those obtained in the case of a HfO_2-SiO_2 system also.[21] However, unlike in the case of (HfO_2-SiO_2) composite thin films,[21] the change in Gd-O bond lengths, oxygen coordination due the incorporation of SiO_2, or evolution of amorphousness decreases monotonically with increase in SiO_2 content in the films and do not show a maximum for 10% SiO_2 content.

IV. SUMMARY AND CONCLUSION

Thus in summary, from the synchrotron-based EXAFS measurements, it has been found that for composite (Gd_2O_3-SiO_2) thin films, oxygen coordination of Gd decreases along with an increase in amorphousness in the samples monotonically with the increase in SiO_2 content in the films. This results in a decrease in the amplitude of the Gd-O peak in the FT-EXAFS spectra of the samples along with a decrease in Gd-O bond length, while AFM measurements show continuous evolution of denser microstructure in the films with an increase in SiO_2 content due to an increase in amorphousness in the samples. It has also been observed that all of the above variations are monotonic with respect to SiO_2 content in the films and do not show any maximum at any particular SiO_2 percentage, as in the case of the HfO_2-SiO_2 composite thin film system.

[1] M. Hong, J. R. Kwo, P.-C. Tsai, Y. Chang, M.-L. Huang, C.-P. Chen, and T.-D. Lin, Jpn. J. Appl. Phys. **46**, 3167 (2007).

[2] M. Hong, M. Passlack, J. P. Mannaerts, J. Kwo, S. N. G. Chu, N. Moriya, S. Y. Hou, and V. J. Fratello, J. Vac. Sci. Technol. **B14**, 2297 (1996).

[3]M. Passlack, M. Hong, J. P. Mannaerts, R. L. Opila, and F. Ren, Appl. Phys. Lett. **69**, 302 (1996).
[4]F. Ren, M. Hong, W. S. Hobson, J. M. Kuo, J. R. Lothian, J. P. Mannaerts, J. Kwo, S. N. G. Chu, Y. K. Chen, and A. Y. Cho, Solid State Electron. **41**, 1751 (1997).
[5]F. Ren, M. Hong, S. N. G. Chu, M. A. Marcus, M. J. Schurman, A. Baca, S. J. Pearton, and C. R. Abernathy, Appl. Phys. Lett. **73**, 3893 (1998).
[6]M. Hong, F. Ren, J. M. Kuo, W. S. Hobson, J. Kwo, J. P. Mannaerts, J. R. Lothian, and Y. K. Chen, J. Vac. Sci. Technol. **B16**, 1398 (1998).
[7]M. Hong, Z. H. Lu, J. Kwo, A. R. Kortan, J. P. Mannaerts, J. J. Krajewski, K. C. Hsieh, L. J. Chou, and K. Y. Cheng, Appl. Phys. Lett. **76**, 312 (2000).
[8]J. Kwo, M. Hong, A. R. Kortan, K. T. Queeney, Y. J. Chabal, J. P. Mannaerts, T. Boone, J. J. Krajewski, A. M. Sergent, and J. M. Rosamilia, Appl. Phys. Lett. **77**, 130 (2000).
[9]A. A. Dakhel, J. Opt. A: Pure Appl. Opt. **3**, 452 (2001).
[10]N. K. Sahoo, M. Senthilkumar, S. Thakur, and D. Bhattacharyya, Appl. Surf. Sci. **200**, 219 (2002).
[11]N. K. Sahoo, S. Thakur, M. Senthilkumar, D. Bhattacharyya, and N. C. Das, Thin Solid Films **440**, 155 (2003).
[12]N. K. Sahoo, S. Thakur, M. Senthilkumar, and N. C. Das, Appl. Surf. Sci. **206**, 271 (2003).
[13]D. Bhattacharyya, A. Biswas, and N. K. Sahoo, Appl. Surf. Sci. **233**, 155 (2004).
[14]N. K. Sahoo, S. Thakur, and M. Senthilkumar, Appl. Surf. Sci. **252**, 1520 (2005).
[15]N. K. Sahoo, R. B. Tokas, and S. Thakur, Appl. Surf. Sci. **253**, 1787 (2006).
[16]N. K. Sahoo, S. Thakur, and R. B. Tokas, Appl. Opt. **45**, 3243 (2006).
[17]N. D. Afify, G. Dalba, U. M. K. Koppolu, C. Armellini, Y. Jestin, and F. Rocca, Mater. Sci. Semicond. Process. **9**, 1043 (2006).
[18]N.D. Afify, G. Dalba, and F. Rocca, J. Phys. D: Appl. Phys. **42**, 115416 (2009).
[19]D. A. Neumayer and E. Cartier, J. Appl. Phys. **90**, 1801 (2001).
[20]J. Moris, L. Miotti, K. P. Bastos, S. R. Teixeira, I. J. R. Baumvol, A. L. P. Rotondaro, J.J. Chambers, M. R. Visokay, L. Colombo, and M. C. Martins Alves, Appl. Phys. Lett. **86**, 212906 (2005).
[21]N. C. Das, N. K. Sahoo, D. Bhattacharyya, S. Thakur, N. M. Kamble, D. Nanda, S. Hazra, J. K. Bal, J. F. Lee, Y. L. Tai, and C. A. Hsieh, J. Appl. Phys. **108**, 023515 (2010).
[22]For more information see http://portal.nsrrc.org.tw/
[23]*Absorptions: Principles, Applications, Techniques of EXAFS, SEXAFS and XANES* edited by D. C. Konigsberger and R. Prince (Wiley, New York, 1988).
[24]A. P. Menushenkov, V. F. Petrunin, V. V. Popov, R. V. Chemikov, A. V. Fedotov, O. V. Kashurnikova, A. A. Yaroslavtsev, and K. V. Klementiev, http://hasyweb.desy.de/science/annual_reports/2007_report/part1/contrib/42/21066.pdf.
[25]Y. Shoujing, W. Feng, W. Yi, Y. Zhimin, T. Hailing, and D. Jun, J. Rar. Earth. **26**, 371(2008).
[26]M. Newville, B. Ravel, D. Haskel, J. J. Rehr, E. A. Stern, and Y. Yacoby, Physica B. **208&209**, 154 (1995).
[27]O. J. Guentert, and R. L. Mozzi, Acta Cryst. **11**, 746 (1958).
[28]D. Lonappan, N. V. Chandra Shekar, P. Ch. Sahu, B. V. Kumarasamy, A. K. Bandyopadhyay, and M. Rajagopalan, Phil. Mag. Lett. **88**, 473 (2008).
[29]For more information, see http://en.wikipedia.org/wiki/Gadolinium(III)_oxide
[30]E. J. Nelson and J. C. Woicik, Appl. Phys. Lett. **76**, 2526 (2000).
[31]T. Nakagawa, T. Osuki, T. A. Yamamoto, Y. Kitauji, M. Kano, M. Katsura, and S. Emura, J. Synchrotron Rad. **8**, 740 (2001).
[32]L. V. Goncharova, M. Dalpointe, D. G. Stardub, T. Giustafsson, E. Garfunkel, P. S. Lysaght, F. J. Barnett, and G. Bersuker, Appl. Phys. Lett **89**, 044108 (2006).
[33]H. Jin, S. K. Oh, H. J. Kang, and M. H. Cho, Appl. Phys. Lett. **89**, 122901 (2006).
[34]M. Ť apajna, A. Rosová, K. Huešková, F. Roozeboom, E. Dobročka, and K. Fröhlich, Microelectron. Eng. **84**, (2007) 2366.
[35]L.-P. Feng, Z. Liu, and Y.-M. Shen, Vacuum **83**, 902 (2009).
[36]D. Cho, C. Min, J. Kim, and S. Oh, Appl. Phys. Lett. **89**, 253510 (2006).
[37]X. G. Tang, H. R. Zeng, A. L. Ding, P. S. Qiu, W. G. Luo, H. Q. Li, and D. Mo, Solid State Commun. **116**, 507 (2000).
[38]S. W. Park, J. M. Choi, K. H. Lee, H. W. Yeom, S. Im, and Y. K. Lee, J. Phys. Chem. B **114**, 5661 (2010).
[39]H. Y. Lee, T. W. Huang, C. H. Lee, and Y. W. Hsieh, Appl. Crystallogr. **41**, 356 (2008).
[40]T. W. Huang, H. Y Lee, Y. W. Hsieh, and C. H. Lee, J. Cryst. Growth **237–239**, 492 (2002).
[41]P. Bhattacharya, T. Komeda, K. Park, and Y. Nishioka, Jpn. J. Appl. Phys. **32**, 4103 (1993).
[42]I. Volintirua, M. Creatorea, J. L. Lindenb, and M. C. M. van de Sandena, Superlattices Microstruct. **39**, 348 (2006).